Modelling and Simulation of Fiber Bragg Grating Characterization for Oil and Gas Sensing Applications

Solomon Udoh, James Njuguma, Radhakrishna Prabhu†
Institute for Innovation, Design and Sustainability
Robert Gordon University
Aberdeen, UK
†Email: r.prabhu@rgu.ac.uk

***Abstract*—In this paper, modelling, simulation and characterization of optical fibre Bragg grating (FBG) for maximum reflectivity for oil and gas sensing applications are presented. The fibre grating length and the refractive index profile are key parameters for effective and high performance optical Bragg grating. The spectral reflectivity, bandwidth and sidelobes were analysed with changes in grating length and refractive index. Modelling and simulation of the Bragg grating which are based on solving the Coupled Mode Theory (CMT) equation by using the transfer matrix method were carried out using MATLAB and the results show that the changes in grating length and refractive index profile affect the bandwidth as the demand for bandwidth and high-speed transmission grows in oil and gas sensing applications.**

Keywords–Fiber Bragg grating (FBG); Reflectivity; Coupled Mode Theory (CMT); Transfer Matrix Method

I. INTRODUCTION

Fiber Bragg grating (FBG) as an important sensing element for measuring multi-parameters measurands such as strain, temperature, pressure and flow has been extensively studied over the past 20 years [1]. FBG has its origin from the discovery of the photosensitivity of germanium-doped silica fiber by Hill et al in 1978 [2, 3]. In 1989, Meltz et al [4] further demonstrated that a permanent refractive index change occurred when a germanium-doped fiber is exposed to direct single photon ultraviolet (UV) light.

FBG is the periodic perturbation of the refractive index along the optical fibre length which is formed by exposing the core of the optical fibre to a periodic pattern of intense UV light [5]. This exposure introduces a permanent change to the refractive index of the core of the fibre. At certain wavelengths, the constructive interference of the reflected band results in a band rejection which is known as the Bragg wavelength [6]. The Bragg wavelength is dependent on the refractive index and the grating period, so any changes on the physical structure on any of these will cause a shift on the Bragg wavelength. This makes the above mentioned parameters to be sensed using the FBG. On this basis, how key parameters affect the quality of the rejected band in FBG is presented.

FBG has been successfully applied in diverse range of areas which include structural health monitoring, telecommunications and chemical sensing [7-11]. For the past 30 years, the oil and gas industry has relied on the use of electronic retrievable sensors that are driven down into the wellbore or reservoir for measurement of key parameters such as temperature, pressure, flow and vibration. Unfortunately, these electronic systems suffer huge limitations such as drastic reduction in reliability, corrosion of electrical parts and susceptibility to electromagnetic interference when used in harsh extreme conditions. Also, the huge number of electronic sensors make the downhole sensing and monitoring application very challenging and complex [12-14]. To optimize the recovery or production efficiency of oil and gas, the industry is gearing towards the implementation of intelligent well and hence there is a need for more sensory capabilities in the wellbore.

The FBG technology is now gaining wide application in oil and gas sensing due the numerous advantages over the electronic sensors which are: electrically passive device (no downhole electronics), intrinsically safe (does not cause explosion when used in harsh environments), high sensitivity, immune to electromagnetic interference (as there are no electrical current flowing at the sensing point), suitable for high temperature operation, distributed sensing capabilities and their relatively small size and light weight [15, 16]. The FGB also have a distinctive advantage over other optical fibre configurations due to its multiplexing capability that allows a single fibre optic cable with tens of gratings to measure a large range of parameters in oil and gas production not limited to downhole production monitoring but also for downstream process monitoring, platform structural monitoring and pipeline monitoring using wavelength division multiplexing (WDM) technique [17].

FBG are generalised distributed reflectors whose characteristic are wavelength-dependent that can accurately be adjusted by proper design. One important feature of the FBG is the relative narrow bandwidth of the reflection spectrum [18]. However, some certain applications such as seismic sensing in the oil and gas industry need large bandwidth [19]. In this paper, using the CMT, a short grating length is needed to achieve a large bandwidth and it was also

978-0-7695-5198-2/14 $31.00 © 2014 Crown Copyright
DOI 10.1109/SIMS.2014.47

found that the refractive index change will also affect the bandwidth.

II. Properties and Principles of FGB Sensing

The refractive index profile, grating length and the grating strength are basically the three qualities that control the properties of FBG. And the properties that need to be control in an FBG are reflectivity, bandwidth and the sidelobe strength. Parameters like strain, temperature and pressure simultaneously act on FBG sensor [20]. The Bragg wavelength of the FBG will vary with changes in any of these parameters experienced by the fibre optic sensor and the corresponding wavelength shifts are as follows:

A. Strain

The shift in Bragg wavelength due to the applied longitudinal strain $\lambda_{B|S}$ is given by [20]

$$\Delta\lambda_{B|S} = \lambda_B(1 - P_e)\varepsilon_z \tag{1}$$

where λ_B is the Bragg wavelength, ε_z is the applied strain along the longitudinal axis and P_e is an effective strain-optic constant defined as

$$P_e = \frac{{n^2}_{eff}}{2}[P_{12} - \upsilon(P_{11} + P_{12})] \tag{2}$$

P_{11} and P_{12} are the components of the fiber optic strain tensor also known as the Pockels constants of the fiber, determined experimentally [21], n_{eff} is the effective refractive index and υ is the Poisson's ratio.

B. Temperature

The shift in Bragg wavelength $\lambda_{B|T}$ as a result of temperature changes ΔT is described by [20]

$$\Delta\lambda_{B|T} = \lambda_B(\alpha + \xi)\Delta T \tag{3}$$

$$\alpha = \frac{1}{\Lambda}(\frac{\partial\Lambda}{\partial T}) \tag{4}$$

$$\xi = \frac{1}{n_{eff}}(\frac{\partial n_{eff}}{\partial T}) \tag{5}$$

where ΔT is the change in temperature, Λ is the grating period, α is the thermal expansion coefficient for the fiber and ξ is the thermo-optic coefficient.

C. Pressure

The shift in Bragg wavelength $\lambda_{B|P}$ as a result of pressure changes ΔP is described by [20, 22]

$$\Delta\lambda_P = \lambda_B[-\frac{(1-2\upsilon)}{E} + \frac{{n^2}_{eff}}{2E}(1-2\upsilon)(2P_{12} + P_{11})]\Delta P \tag{6}$$

where E is the Young's modulus of the fibre. Equation 6 shows the wavelength shift and is directly proportional to the pressure change ΔP.

III. Models of FBG

A. Coupled Mode Theory (CMT)

To model the FBG, the CMT will be considered since it is one of the best tools in understanding the optical properties of gratings. The CMT is a powerful mathematical tool to analyze the wave propagation and interactions with materials in optical waveguide. The CMT sees the grating structure as perturbation to an optical waveguide [23]. CMT have been used to successfully model numerous fibre grating structures and the results show excellent match with experimental works. The fabrication of FBG results in a perturbation on the effective refractive index n_{eff} of the guided modes which is given by [6]

$$\delta n_{eff}(z) = \bar{\delta n_{eff}}(z)\{1 + \nu\cos[\frac{2\pi}{\Lambda}z + \phi(z)]\} \tag{7}$$

where $\bar{\delta n_{eff}}$ is the 'dc' index change, ν is the fringe visibility of the index change, Λ is the grating period and $\phi(z)$ denotes the grating chirp. For a single mode FBG, the simplified coupled mode equations are given as [6]

$$\frac{dR}{dz} = i\hat{\sigma}R(z) + i\kappa S(z) \tag{8}$$

$$\frac{dS}{dz} = -i\hat{\sigma}S(z) - i\kappa^* R(z) \tag{9}$$

where $R(z)$ and $S(z)$ are the amplitudes of forward-propagating and backward-propagating modes respectively. κ is the "ac" coupling and $\hat{\sigma}$ is the general 'dc' coupling coefficient. They are defined as

$$\hat{\sigma} = \delta + \sigma - \frac{1}{2}\frac{d\phi}{dz} \tag{10}$$

$$\kappa = \kappa^* = \frac{\pi}{\lambda}\nu\bar{\delta n_{eff}} \tag{11}$$

The detuning δ and σ in Equation 10 are defined as

$$\delta = \beta - \frac{\pi}{\Lambda} = 2\pi n(\frac{1}{\lambda} - \frac{1}{\lambda_D}) \tag{12}$$

$$\sigma = \frac{2\pi}{\lambda}\bar{\delta n_{eff}} \tag{13}$$

For a uniform FBG, in which β is the mode propagation constant, δn_{eff} is a constant and the grating chirp $\frac{d\phi}{dz} = 0$, and thus κ,σ and $\hat{\sigma}$ in Equations 10, 11 and 13 are constants. By specifying the appropriate boundary conditions, the analytical expression of the reflectivity is obtained as [6]

$$r = \frac{\sinh^2(\sqrt{\kappa^2 - \hat{\sigma}}L)}{\cosh^2(\sqrt{\kappa^2 - \hat{\sigma}}L) - \frac{\hat{\sigma^2}}{\kappa^2}} \tag{14}$$

The transfer matrix method is applied to solve the coupled mode theory equations and to obtain the spectral response of FBG. The FBG with grating length L is divided into sections

Figure 1. The transfer matrix method applied to obtain the spectral characteristics of a FBG.

of M as shown in Figure 1 and the larger the number of M, the more accurate this method is. During design, care should be taken not to make M arbitrary too large as the coupled mode theory is difficult to implement for a uniform grating section with just few periods long [24].

The amplitude of the forward-propagation mode and the backward-propagation mode before and after the i^{th} uniform sections are represented in a matrix of the form F_i as;

$$\begin{bmatrix} R_i \\ S_i \end{bmatrix} = F_i \begin{bmatrix} R_{i-1} \\ S_{i-1} \end{bmatrix} = \begin{bmatrix} F_{11} & F_{12} \\ F_{21} & F_{22} \end{bmatrix} \begin{bmatrix} R_{i-1} \\ S_{i-1} \end{bmatrix} \tag{15}$$

where R_i and S_i are the amplitudes of the forward-propagation mode and backward-propagation mode after the i^{th} uniform sections and R_{i-1} and S_{i-1} are the amplitudes of the forward-propagation mode and backward-propagation mode before the i^{th} uniform sections. The elements in the transfer matrix are represented as;

$$F_{11} = F^*{}_{22} = cosh(\gamma_B \Delta z) - i\frac{\hat{\sigma}}{\gamma_B} sinh(\gamma_B \Delta z) \tag{16}$$

$$F_{11} = F^*{}_{22} = -i\frac{\kappa}{\gamma_B} sinh(\gamma_B \Delta z) \tag{17}$$

where Δz is the length of the i^{th} uniform section, $\gamma_B = \sqrt{\kappa^2 - \hat{\sigma}}$ is the imaginary part for which $|\hat{\sigma}| > \kappa$ [6] , and * represent the complex conjugate. The output amplitude are obtained by multiplying all the matrices for individual sections as

$$\begin{bmatrix} R_M \\ S_M \end{bmatrix} = F \begin{bmatrix} R_0 \\ S_0 \end{bmatrix} \tag{18}$$

where $F = F_M.F_{M-1}...F_1$.

The output amplitudes for the non-uniform FBG are obtained by applying the boundary conditions, $R_0 = R(L) = 1$ and $S_0 = S(L) = 0$. The amplitude reflection coefficient $\rho = R_M/S_M$, and the power reflection $r = |\rho|^2$ are calculated by the transfer matrix method.

IV. Results and Analysis

The spectral response of a uniform FBG is obtained, the simulation was carried out using MATLAB and the parameters of the uniform FBG used for the simulation are listed in Table 1.

TABLE I
Simulation Parameters of FBG

Parameters	Symbols	Values
Effective refractive index	n_{eff}	1.447
Grating length changes	L	1 - 8 mm
Bragg wavelength	λ_B	1550 nm
Change in refractive index	δ_n	0.0005 - 0.002
Grating period	Λ	535.59 nm

A. Spectral reflectivity dependence on grating length

The spectral response of a uniform FBG is affected as the length of the grating is altered by external perturbation such as strain, temperature and pressure. The dependency of spectral reflectivity on different grating lengths were observed and analysed by varying the grating length from $1 - 10$ mm. Figure 2 shows the simulated results of the reflectivity as a function of wavelength for different lengths of the grating. Clearly from the graphs, the reflectivity of the uniform FBG increases with increase in the grating length. When the grating length $L = 1$ mm, 2 mm, 3 mm, 4 mm and 5 mm the maximum reflectivity is 58.83%, 93.28%, 99.09%, 99.88% and 99.98% respectively. At $L = 6$ mm, the reflectivity reaches 100%. When the grating length is increased further to $L = 10$ mm, it is observed that the maximum reflectivity maintains at 100%.

Figure 3 shows a linear relationship between the change in grating length and the shift in centre wavelength. It is observed from the graph, as the grating length changes, there is a corresponding shift in the centre wavelength.

B. Spectral Reflectivity Dependence on Refractive Index

Figure 4 shows the results of the simulation of a uniform FBG with grating length of $L = 1$ mm as the change in refractive index is varied from $\delta_n = 0.0005 - 0.002$. For grating with refractive index of $\delta_n = 0.0005$, 0.0006, 0.0007, 0.0008, 0.0009 and 0.001 the maximum reflectivity is 58.83%, 70.28%, 79.07%, 85.51%, 90.09% and 99.01% respectively. 100% maximum reflectivity was achieved at $\delta_n = 0.002$ and maintains this value when the refractive index is further increased. Figure 5 shows the linear relationship between the refractive index change and the shift in centre wavelength. As the change in refractive index increases, there is a corresponding increase in the centre wavelength which is in agreement with the findings of Sunita and Mishra [25]. The shifts in centre wavelength is used for calculating the external perturbations like strain, temperature, pressure etc.

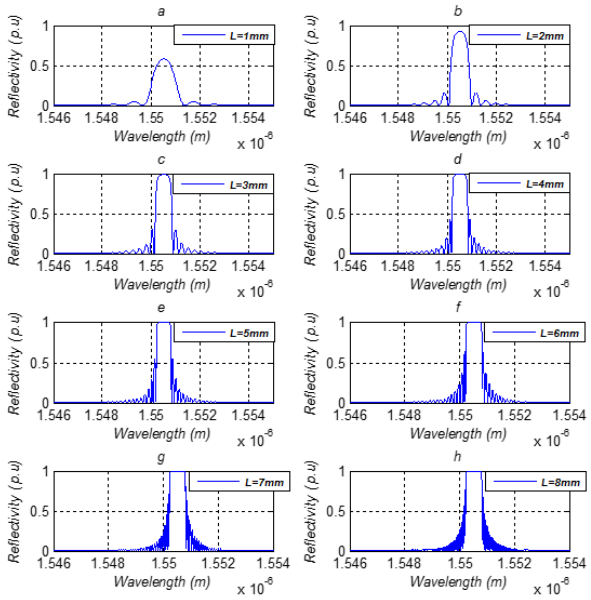

Figure 2. Spectral reflectivity characteristics of FBG for different grating lengths 1 - 8 mm from a to h

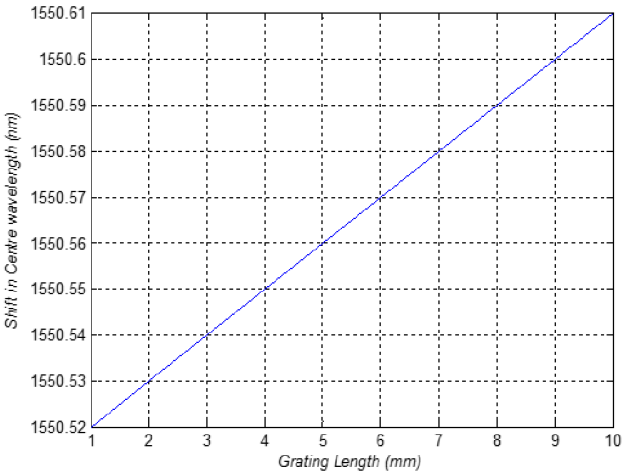

Figure 3. Effect of grating length on FBG

C. Bandwidth dependence on grating length and refractive index

The dependence of bandwidth on grating length was observed and analysed, the bandwidth values of a FBG with different grating lengths were calculated from Figure 2 and plotted in Figure 6. It can be observed that the bandwidth reduces with increase in grating length but increases with increase in change in refractive index of a FBG.

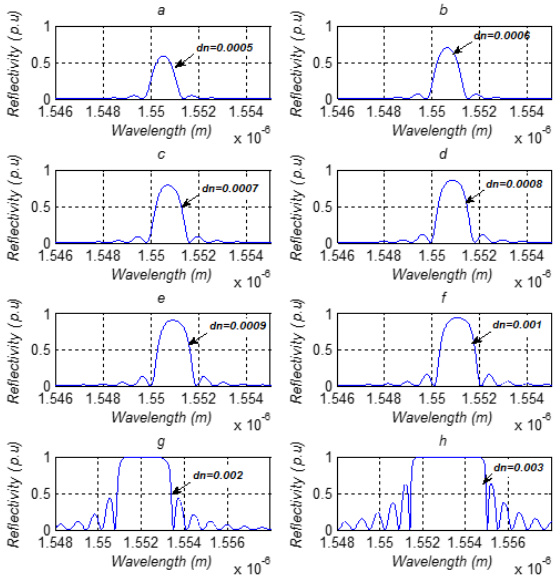

Figure 4. Spectral reflectivity characteristics of FBG for different refractive index change $0.0005 - 0.003$ from a to h

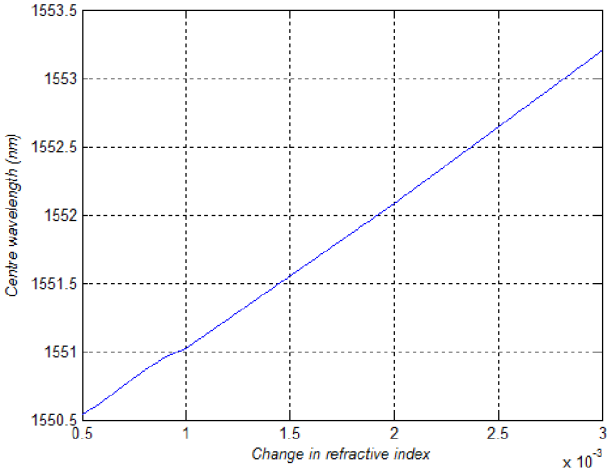

Figure 5. Effect of refractive index change on centre wavelength

In Figure 6, it can be seen that when the grating length is 5 mm with a refractive index change of 0.0005 the bandwidth is 0.6 nm. As the grating length reduces to 2 mm, the bandwidth increases to 0.75 nm. Theoretically, larger bandwidth of a FBG can be achieved with smaller grating length. Thus, for a strong grating with a large bandwidth to be achieved, the grating length has to be small and the refractive index change must be large. However, for a strong grating with smaller bandwidth, the grating

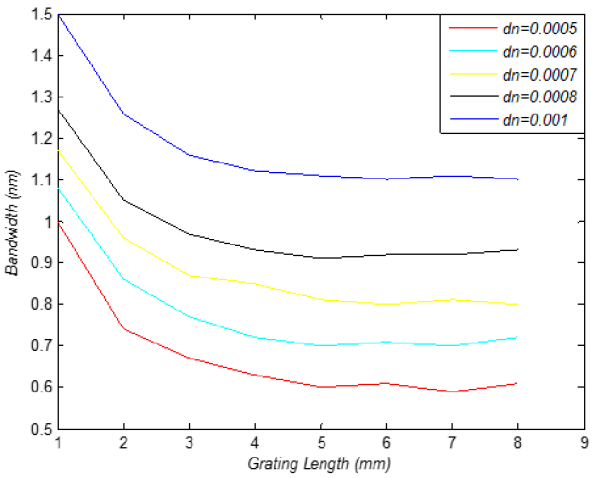

Figure 6. Effect of grating length on bandwidth for different refractive index change $0.0005 - 0.001$

length must be long and the refractive index change must be small. Also, it is worth noting that the strength of the sidelobes in the reflection spectrum increases with increase in both the grating length and the change in refractive index as indicated in Figure 2 and Figure 4. The sidelobes are undesirable since they could cause channels crosstalk (interference between channels) and they are suppress by method known as apodization [26].

V. Conclusion

Using the coupled mode theory, a larger bandwidth can be achieved with short grating length by proper design. The modelling, simulation and characterization of optical FBG were presented. The spectral reflectivity, bandwidth and sidelobes were analysed with changes in grating length and refractive index. The reflectivity increases with increase in grating length and refractive index change. The bandwidth of FBG decreases by increasing the grating length and it increases by increasing the refractive index change. The strength of the sidelobes increases with increase in the grating length and the refractive index change which can be suppressed by apodization. These analyses give better understanding of the relationships of FBG characterization and suggest possible ways of designing high performance FBG sensors for oil and gas applications.

Acknowledgment

The authors would like to sincerely thank Petroleum Technology Development Fund (PTDF) for funding this research and their continued support.

References

[1] A. Kersey, M. A. Davis, H. J. Patrick, M. Leblanc, K. P. Koo, C. G. Askins, M. A. Putnam, and E. J. Friebele, *"Fiber grating sensors,"* Lightwave Technology, Journal of, vol. 15, pp. 1442-1463, 1997.

[2] K. O. Hill, Y. Fujii, D. C. Johnson, and B. S. Kawasaki, *"Photosensitivity in optical fiber waveguides: Application to reflection filter fabrication,"* Applied Physics Letters, vol. 32, pp. 647-649, 1978.

[3] B. S. Kawasaki, K. O. Hill, D. C. Johnson, and Y. Fujii, *"Narrow-band Bragg reflectors in optical fibers,"* Optics Letters, vol. 3, pp. 66-68, 1978.

[4] G. Meltz, W. W. Morey, and W. H. Glenn, *"Formation of Bragg gratings in optical fibers by a transverse holographic method,"* Optics Letters, vol. 14, pp. 823-825, 1989.

[5] A. Othonos, *"Fiber Bragg gratings,"* Review of Scientific Instruments, vol. 68, pp. 4309-4341, 1997.

[6] T. Erdogan, *"Fiber grating spectra,"* Lightwave Technology, Journal of, vol. 15, pp. 1277-1294, 1997.

[7] P. Antunes, H. Lima, N. Alberto, L. Bilro, P. Pinto, A. Costa, H. Rodrigues, J. L. Pinto, R. Nogueira, H. Varum, and P. S. Andr, *"Optical Sensors Based on Fiber Bragg Gratings for Structural Health Monitoring,"* in New Developments in Sensing Technology for Structural Health Monitoring. vol. 96, S. Mukhopadhyay, Ed: Springer Berlin Heidelberg, pp. 253-295, 2011.

[8] A. D. Kersey, *"A Review of Recent Developments in Fiber Optic Sensor Technology,"* Optical Fiber Technology, vol. 2, pp. 291-317, 1996.

[9] A. D. Kersey, M. A. Davis, T. A. Berkoff, D. G. Bellemore, K. P. Koo, and R. T. Jones, *"Progress toward the development of practical fiber Bragg grating instrumentation systems,"* Proc. SPIE, Fiber Optic and Laser Sensors XIV pp. 40-63 1996.

[10] G. Meltz, *"Overview of fiber grating-based sensors,"* Proc. SPIE 2838, Distributed and Multiplexed Fiber Optic Sensors VI, pp. 2-22. 1996.

[11] O. S. Wolfbeis, *"Fiber-Optic Chemical Sensors and Biosensors,"* Analytical Chemistry, vol. 76, pp. 3269-3284, 2004.

[12] W. A. Nestlerode, *"The Use Of Pressure Data From Permanently Installed Bottom Hole Pressure Gauges,"* SPE Conference, 27-28 May, Denver, Colorado, 1963

[13] A. C. Gringarten, T. von Schroeter, T. Rolfsvaag, and J. Bruner, *"Use of Downhole Permanent Pressure Gauge Data to Diagnose Production Problems in a North Sea Horizontal Well,"* SPE Conference, 2003

[14] T. Unneland, *"Permanent Downhole Gauges Used in Reservoir Management of Complex North Sea Oil Fields,"* SPE, 1994.

[15] K. T. V. Grattan and T. Sun, *"Fiber optic sensor technology: an overview,"* Sensors and Actuators A: Physical, vol. 82, pp. 40-61, 2000.

[16] A. D. Kersey, J. R. Dunphy, and A. D. Hay, *"Optical Reservoir Instrumentation System."* Offshore Technology Conference, vol. 2, pp. 469-472, 1998

[17] A. D. Kersey, T. A. Berkoff, and W. W. Morey, *"Multiplexed fiber Bragg grating strain-sensor system with a fiber Fabry-Perot wavelength filter,"* Optics Letters, vol. 18, pp. 1370-1372, 1993.

[18] S. Shaari and S. Mah Chee, *"Characteristics of large bandwidth fiber Bragg grating with short grating length,"* in Semiconductor Electronics, 2000. Proceedings. ICSE 2000. IEEE International Conference on, pp. 203-206, 2000.

[19] W. Ecke, K. H. Jckel, J. Schauer, and R. Willsch, *"High Temperature Interferometric Displacement Measuring System for Fibre Optic Seismic Sensors in Deep Borehole Applications,"* in Optical Fiber Sensors, Sapporo, Japan, 1996.

[20] A. Othonos and K. Kalli, *Fiber Bragg gratings: fundamentals and applications in telecommunications and sensing:* Artech House, 1999.

[21] A. Bertholds and R. Dandliker, *"Determination of the individual strain-optic coefficients in single-mode optical fibres,"* Lightwave Technology, Journal of, vol. 6, pp. 17-20, 1988.

[22] G. B. Hocker, *"Fiber-optic sensing of pressure and temperature,"* Applied Optics, vol. 18, pp. 1445-1448, 1979.

[23] W. P. Huang, *"Coupled-mode theory for optical waveguides: an overview,"* Journal of the Optical Society of America A, vol. 11, pp. 963-983, 1994.

[24] M. Yamada and K. Sakuda, *"Analysis of almost-periodic distributed feedback slab waveguides via a fundamental matrix approach,"* Applied Optics, vol. 26, pp. 3474-3478, 1987.

[25] S. P. Ugale and V. Mishra, *"Optimization of fiber Bragg grating length for maximum reflectivity,"* in Communications and Signal Processing (ICCSP), 2011 International Conference on, 2011, pp. 28-32.

[26] J. Albert, K. O. Hill, B. Malo, S. Theriault, F. Bilodeau, D. C. Johnson, and L. E. Erickson, *"Apodisation of the spectral response of fibre Bragg gratings using a phase mask with variable diffraction efficiency,"* Electronics Letters, vol. 31, pp. 222-223, 1995.